45th AIAA Aerospace Sciences Meeting and Exhibit
8 - 11 January 2007, Reno, Nevada

AIAA 2007-1121

Control of the Spanwise Distribution of Circulation on NACA 0012 and Flat Plate Wings

D. Williams*, S. Doshi†, J. Collins‡
Illinois Institute of Technology, Chicago, IL

T. Colonius§
California Institute of Technology, Pasadena, CA

Open-loop active flow control is used to modify the spanwise distribution of circulation around an NACA 0012 and flat plate wing. The leading edge on both airfoils and tip regions of the NACA airfoil contain spatially localized actuators that can be independently controlled in terms of amplitude and frequency, allowing the spanwise distribution of circulation to be modified. Different orientations of the pulsed-blowing actuators were used to provide upstream, downstream, in-line with the flow, and outward span components of actuation. The actuation effectiveness was documented using force balance measurements of the lift and drag, smoke-wire visualization, surface pressure measurements and PIV velocity field measurements. Actuation with an upstream component is shown to be far more effective in reducing the separated region than actuation in the streamwise direction. Initial measurements of the change in circulation on the suction surface of the airfoil indicate that spatially localized forcing produces global changes over the wing, primarily associated with the reduction in size of the separated flow region.

Nomenclature

AR	=	aspect ratio
b	=	wing span
c	=	wing chord
C_L	=	wing lift coefficient
C_p	=	pressure coefficient
C_μ	=	actuator momentum coefficient
d_{jet}	=	actuator jet diameter
f	=	forcing frequency
F^+	=	dimensionless forcing frequency, $F^+ = fc/U_\infty$
U,V	=	x, y components of mean velocity
Q	=	velocity magnitude, $Q = \sqrt{U^2 + V^2}$
Re_c	=	Reynolds number based on chord
t	=	airfoil thickness
x	=	coordinate in flow direction
y	=	coordinate in direction of the airfoil span
z	=	vertical coordinate normal to chord
α	=	angle of attack
ΔC_L	=	lift increment, $C_{Lactuated} - C_{Lbaseline}$
$\Gamma_{\alpha 0}$	=	circulation on suction surface of airfoil at $\alpha=0^o$

* Professor, MMAE Dept., Illinois Institute of Technology, 3110 S. State St., Chicago IL, AIAA Associate Fellow.
† Graduate Research Assistant , MMAE Dept., Illinois Institute of Technology, 3110 S. State St., Chicago IL, 60616
‡ Graduate Research Assistant , MMAE Dept., Illinois Institute of Technology, 3110 S. State St., Chicago IL, 60616
§ Professor, Mechanical Engineering Dept., California Institute of Technology, Pasadena, CA, 91125

I. Introduction

The objective of this experiment is to explore the ability of active flow along the leading edge and tip region of finite span wings to modify the leading-edge and tip vortex (LEV/TV) system. The longer term goal is to extend the range of aspect ratios and Reynolds numbers for which steady lift can be maintained at very high angles of attack (AOA), while realizing benefits associated with higher aspect ratio aerodynamics during cruise. Control of the leading edge vortex is expected to enhance maneuverability by stabilizing or synchronizing vortex shedding during pitch, yaw, and roll, and in response to gusts. The premise for leading-edge and tip vortex control is based on biological fliers. Insect wings are remarkable for their ability to stabilize the LEV that prevents stall at high angle of attack, but without active flow control that stability appears to be limited to an aspect ratio < 3 and Reynolds number (Re) $\leq 10^4$. There is a strong interplay between the tip vortex and leading edge vorticity generation[1], and in all flapping flight, vortex shedding is carefully synchronized to regulate aerodynamic forces. Similarly, previous work in open-loop separation control at high Re shows that pulsed air injection can lead to more organized vortex shedding that results in higher lift and smaller mean separation bubbles. However, open-loop performance deteriorates subject to disturbances that desynchronize the actuation-shedding phase lock. Ultimately to robustly exploit these high-lift mechanisms, closed-loop controllers will use sensors to track the estimated circulation and position of LEV, and apply control based on low-order models of the fluid dynamics of flow over the wings. An overview of the project can be found in the article by Colonius, et al.[2]

Figure 1. IIT – Fejer unsteady flow wind tunnel.

The concept of lift augmentation by spanwise blowing was studied by Dixon[3], who showed that the leading edge vortex could be prevented from shedding when a jet of air was blown laterally over the suction surface of the airfoil. Spanwise blowing was speculated to create sweep effects, similar to delta-wings. Dixon used a single jet positioned near the root of the wind and at the c/4 location on a rectangular flat-plate wing with aspect ratio 4.7. Steady blowing with momentum coefficients from C_μ = 0.29 to 0.82 increased the maximum lift coefficients from C_L = 1.3 to 2.5.

Here we explore the possibility of achieving a similar stabilization of the leading edge vortex, by adding a spanwise component to the pulsed-blowing jets from actuators distributed along the leading edge and tip regions of the test airfoils. The response of the airfoil flow to individually controlled actuators with open loop forcing is being documented to provide the background information needed to develop a closed loop control model. A particularly important measurement was to determine the degree of influence the pulsed-blowing actuators will have on the spanwise circulation distribution.

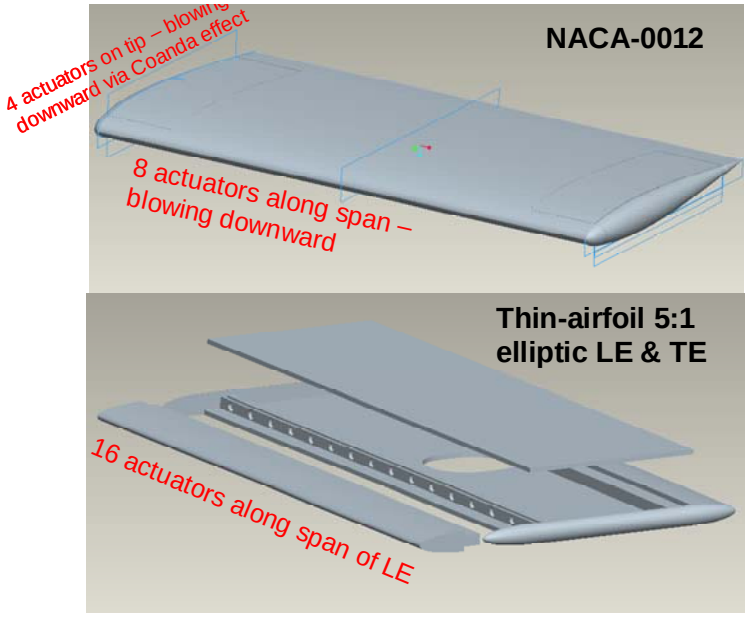

Figure 2. Airfoil models with aspect ratioAR = 2.

II. Experimental Setup

The leading edge and tip vortex interaction studies are being conducted under steady and dynamic conditions in the Andrew Fejer Unsteady Flow Wind Tunnel shown in Fig. 1. The test section cross-section is .61m by .61. Chord Reynolds numbers can be varied from Re_c = 30,000 to 1,000,000. A computer controlled shutter at the downstream end of the test section allows the freestream speed to be modulated at frequencies up to 4 Hz. The wind tunnel fan speed and shutter mechanism are controlled with a feedback tracking algorithm developed by Professor Rowley at Princeton University. With this system it is possible to simulate variations in flight speed during complex maneuvers.

The two airfoil models used in the experiments were mounted on a sting connected to a force balance and pitching mechanism. The NACA 0012 and flat plate airfoils had a chord c = 203mm, span b = 406mm, and aspect ratio AR = 2. The flat plate airfoil had a thickness of 14 mm (.56 in.) giving a thickness ratio t/c=0.07. A 5:1 elliptic leading and trailing edges were used similar to the design of Torres and Mueller[4]. Both airfoils are shown in Fig. 2. Actuation of the NACA 0012 consisted of four pulsed-blowing slots positioned along each wing tip, and eight slots located along the leading edge. Each actuator was isolated from its neighbor, and could be individually activated. For the flat plate (thin airfoil), 16 actuators were located along the leading edge. The leading edge was modular, and could be exchanged with other leading edges to change the direction of actuation. A drawing of the leading edge for upstream blowing configuration is shown in Fig. 3. The diameter of each actuator jet hole was 0.79 mm (0.031in.), and angled 10° upward from the chord line of the airfoil. Straight-blowing actuation used jets aligned with the flow, whereas, outward blowing actuation used the same configuration as shown in Fig. 3, with the addition of a 45° spanwise component to the jets. The four configurations used with the flat-plate airfoil are sketched in Fig. 4.

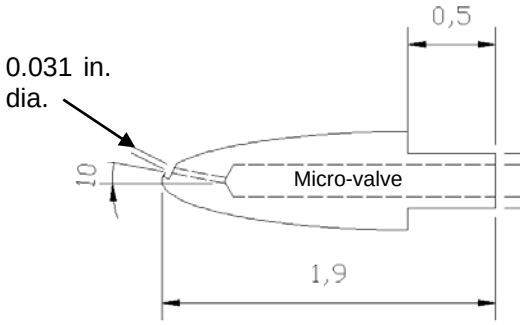

Figure 3. Nose section for upstream actuation (dimensions are in inches.)

When pulsed-blowing actuation was used, there were two forcing frequencies of interest; namely, a low frequency at F^+=0.67 (~ 5 Hz) corresponding to the global instability of the separated flow region, and a high frequency (F+ =2) associated with the Kelvin-Helmholtz instability of the separated shear layer.

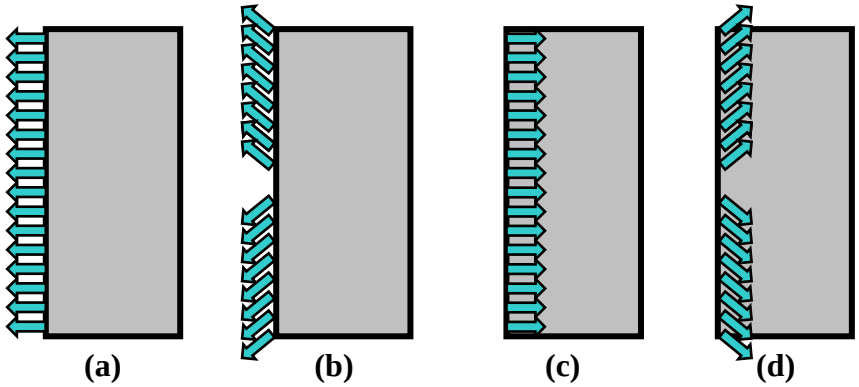

Figure 4. Planview of actuation configurations used on flat plate airfoil. a) upstream straight; b) upstream outward span; c) downstream straight; d) downstream outward span.

Downstream blowing actuators used the same leading edge, with the addition of a thin piece of brass shim stock attached to the leading edge lip. The shim acted to redirect the actuator jet in the downstream direction, tangent to the top surface. The effect of the modification (without flow through the actuators) on the lift and drag coefficients is shown in Fig. 5.

The structure of the separated flow region was mapped using a two-component digital PIV from IDT, Inc. Overall force and moment measurements were obtained with an ATI Nano-17 force balance system.

III. ActuatorCalibration

The flow rate through individual actuators was measured using two independent flow measuring instruments, a Meriam Instruments laminar flow element model 50MJ10 (LFE), and a Singer model DTM-200 dry test meter. The LFE measures the flow rate by measuring the differential pressure across an orifice, whereas, the dry test meter is a totalizing flow meter that records the volume of fluid passed through it in a given time. Air was supplied to the actuator through the laminar flow element, while the dry test meter was connected to the outlet of the actuator.

Actuators were also calibrated with a hot-wire anemometer in combination with the dry test meter. In this case all 16 actuators were connected inside the flat plate wing. Air to the actuators was supplied through a single settling chamber inside the wing. The settling chamber was supplied by four 3.2 mm (0.125 in.) diameter air supply lines. The supply line pressure was measured with a Wallace & Tiernan 241 kPa (35 psig) pressure gauge.

Hot-wire measurements were done with a shim on the nose piece creating a downstream flow. The hot-wire sensor was placed approximately 3 mm from the exit of the actuator slot, and traversed across to locate the position of maximum velocity. Additional hot-wire measurements were done at the location of maximum velocity, while varying the supply pressure to the actuators.

A dry test meter was connected between the air supply line and the pressure gauge to measure the total flow rate supplied to the actuators. These tests were carried out for both steady and pulsed blowing. For pulsed blowing, the total flow rate measured with the dry test meter was halved, since with a 50 percent duty cycle only half the air supplied to the actuators actually contributed to the momentum addition to the flow, while the remaining air was vented back through the sting when the micro-valves were closed. The momentum coefficient was calculated using a jet area based on d_{jet} = 0.79 mm (1/32 in.) as

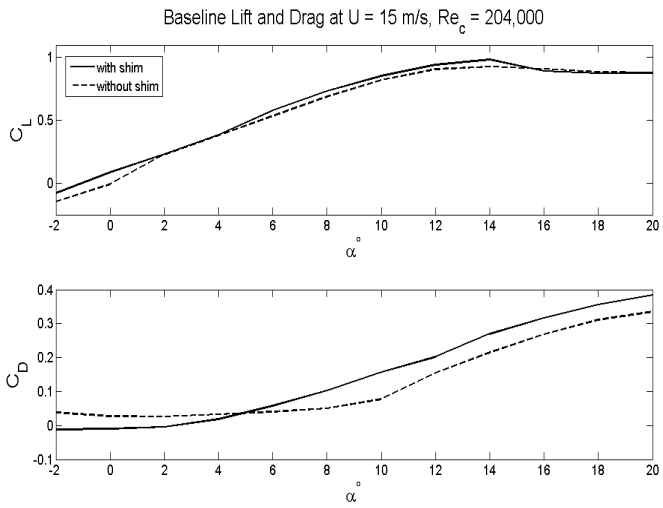

Figure 5. Baseline lift and drag for flat-plate (thin) airfoil with and without shims to redirect the actuator jet.

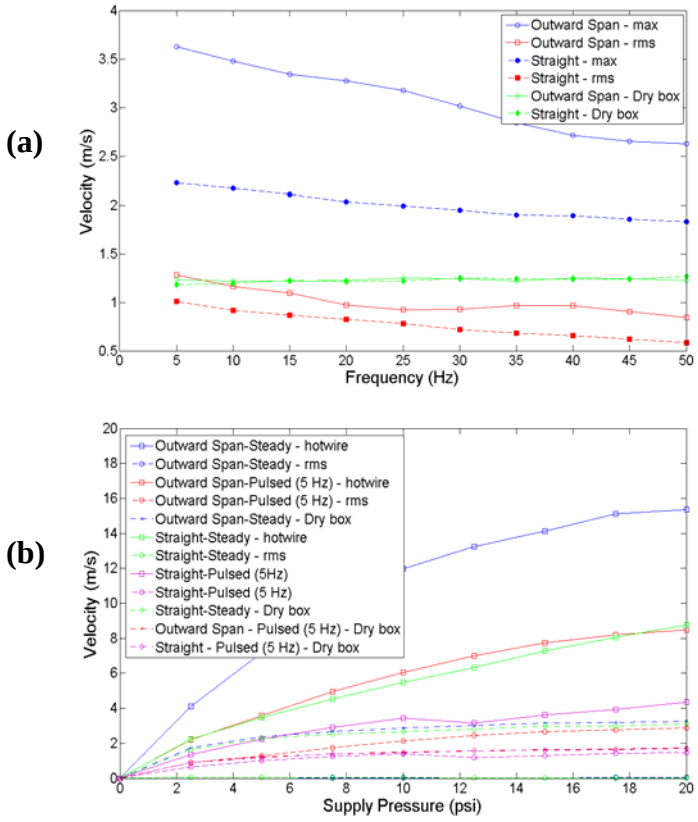

Figure 6. (a) Actuator velocity dependence on forcing frequency. Two leading edge actuators are shown: downstream-straight and downstream-outward blowing. (b) velocity dependence on supply pressure.

the diameter for each of the 16 actuator exit holes on the wing.

Fig.6b shows mean and r.m.s. velocities exiting the actuator as the supply pressure is increased. As expected the velocity increases as the square-root of the supply pressure.

IV. Results from Open-Loop Forcing Tests

A. Comparison of upstream and downstream actuation

The baseline lift and drag measurements shown in Fig. 5 indicate that stall on the flat plate airfoil begins at $\alpha = 14^o$. The stall is actually a gradual process that develops from a trailing-edge separated flow region, beginning at the mid-span and then spreading in the upstream and spanwise directions as the angle of attack increases. Similar behavior was observed with the NACA 0012 airfoil. By an angle of attack of 16^o the mid-span region of the flat plate airfoil is fully separated, but only partially separated near the tip regions.

The separated flow region is visible in the smoke-wire images shown in Figs. 7a and 7b. Figure 7a shows the flow at the mid-span of the airfoil, and Fig. 7b shows the ¼-span location. The separated region is highly unsteady, and two large vortices are visible in the shear layer.

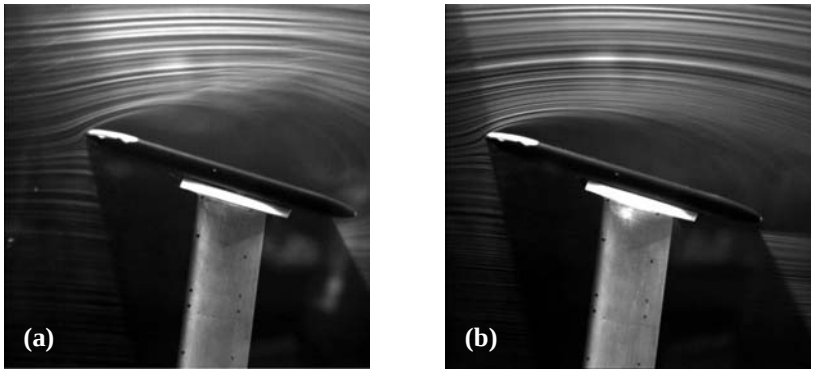

Figure 7. Smoke wire visualizations of baseline flow (no forcing) over flat-plate airfoil at $\alpha = 16^o$; (a) y/(b/2) = 0; (b) y/(b/2) = 0.5.

The effect of upstream forcing with steady-blowing actuators is shown in Fig. 8, with Fig. 8a and 8b corresponding to the mid-span and ¼-span locations, respectively. The size of the separation region is visibly smaller in Fig. 8b with actuation, while the mid-span visualization shows unsteadiness with smaller scale vortices in comparison to the baseline case. The ¼-span location appears to be almost fully attached in Fig. 8b once the active flow control is activated. There also appears to be a reduction in the amount of large-scale turbulence.

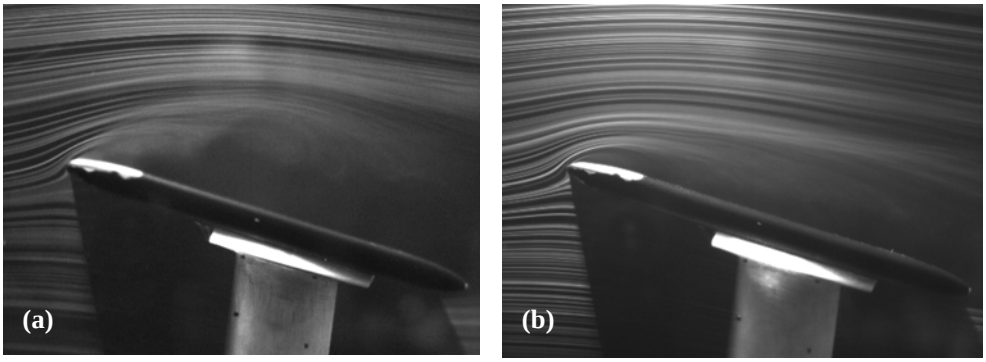

Figure 8. Smoke wire visualizations with upstream, straight, steady-flow actuation over a flat-plate airfoil at $\alpha = 16^o$; (a) y/(b/2) = 0; (b) y/(b/2) = 0.5.

A more quantitative measure of the effect of upstream actuation on the separated region comes from the PIV measurements shown in Figs. 9a-d. The size of the recirculation region is decreased with steady blowing, as can be seen by comparing the streamlines, but has not been completely eliminated. This is consistent with the flow visualization images at the mid-span. The center of the recirculation appears as a focus in the streamline patterns, which we believe is the result of a strong spanwise component of flow in the recirculation region.

The maximum values of negative Reynolds stress (u'v') are found near the dividing streamline over the separated flow region, and indicate a transfer of energy from the mean flow into the turbulent flow. In the actuated case (Fig. 9b) the Reynolds stress shows a strong positive value near the leading edge, possibly associated with the strong favorable pressure gradient in the leading edge region. Comparison of Figs. 9c and 9c show that the upstream actuation accelerates the formation of the negative Reynolds stress region, resulting in the elimination of the recirculation region.

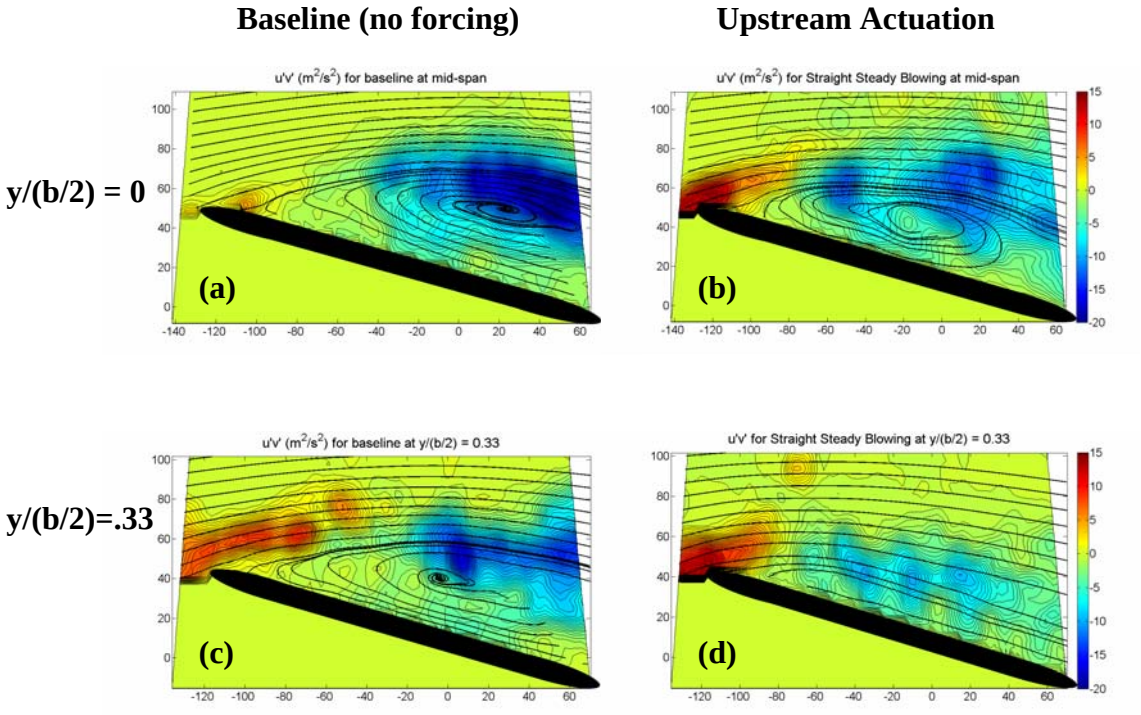

Figure 9. Arbitrary streamlines and Reynolds stress contours for the baseline and upstream forcing cases at the mid-span and y/(b/2) = 0.33 span of the flat plate airfoil. Reynolds stress contour levels range from -20 m^2/s^2 (blue) to +15 m^2/s^2 (red.) The amplitude of the steady blowing was C_μ = 8.3 x 10^{-5} percent. The x and y axis labels are in millimeters. a) baseline, y/(b/2)=0; b) upstream actuation, y/(b/2)=0; c) baseline, y/(b/2) = 0.33; d) y/(b/2) = 0.33.

Measurements of the overall lift and drag were obtained with a six-component force balance. The effects of upstream and downstream actuation on lift with steady and pulsed blowing are shown as a lift increment $\Delta C_L = C_{L\_actuated} - C_{L\_baseline}$ in Fig. 10. The error bars shown are based on the maximum variations observed after repeating the experiments. Downstream oriented actuation is a common configuration used in active flow control, and the values of the momentum coefficient (C_μ ~ .01 percent) required to enhance the lift are typical of those observed by other investigators. Lift is gradually and continuously increased as the momentum coefficient is increased. The lift does not appear to saturate with downstream directed actuation, and presumably larger forcing amplitudes would result in higher C_L values.

A significantly different response of the lift coefficient is seen with the upstream actuation, shown in Fig. 10b. A close-up of the rapid change in C_L is shown in Fig. 10c. The maximum increase in lift occurred at very low amplitude forcing and saturated almost immediately. The lowest resolvable supply pressure with our control system pressure regulator was 860Pa (0.125 psig). The maximum lift increment occurred at 1.72 kPa (0.25 psig) corresponding to $C_\mu = 8.3x10^{-5}$ percent, which is two orders of magnitude lower than that achieved with downstream

actuation. While this is a very encouraging result, suggesting that forces on an airfoil may be controlled with extremely low forcing amplitudes, we caution that the reasons for the upstream actuation efficiency are not fully understood yet. We cannot be certain that the results will translate to cambered airfoils, or airfoils with a different leading-edge configuration. Furthermore, the PIV and smoke visualizations show that the saturated state with upstream actuation does not completely eliminate the flow separation in the mid-span region of the airfoil.

Four different types of actuation are shown in Fig. 10; namely, (1) steady-straight, (2) steady-outward, (3) pulsed-straight and (4) pulsed-outward, where straight refers to being along the x-axis and outward indicates a 45^{o} angle toward the tips of the airfoil as previously indicated in Fig. 4. The effects of the four types of downstream-oriented actuation are shown in Fig. 10a, where it can be seen that the outward-span pulsed blowing at f=5Hz (F^{+}=.067) is the most effective at increasing the lift coefficient. However, when upstream actuation is used, then straight-steady actuation is the most effective at the low amplitudes and outward-steady becomes more effective at the higher forcing amplitudes.

Figure 11a-b show the effect of outward span, steady blowing on the suction surface flow field at C_{μ}= 8.3x10^{-5} percent. Eight planes of PIV measurements of the U-component of velocity are shown. An iso-surface corresponding to 11 m/s is superposed on the data to identify changes in the separated region.

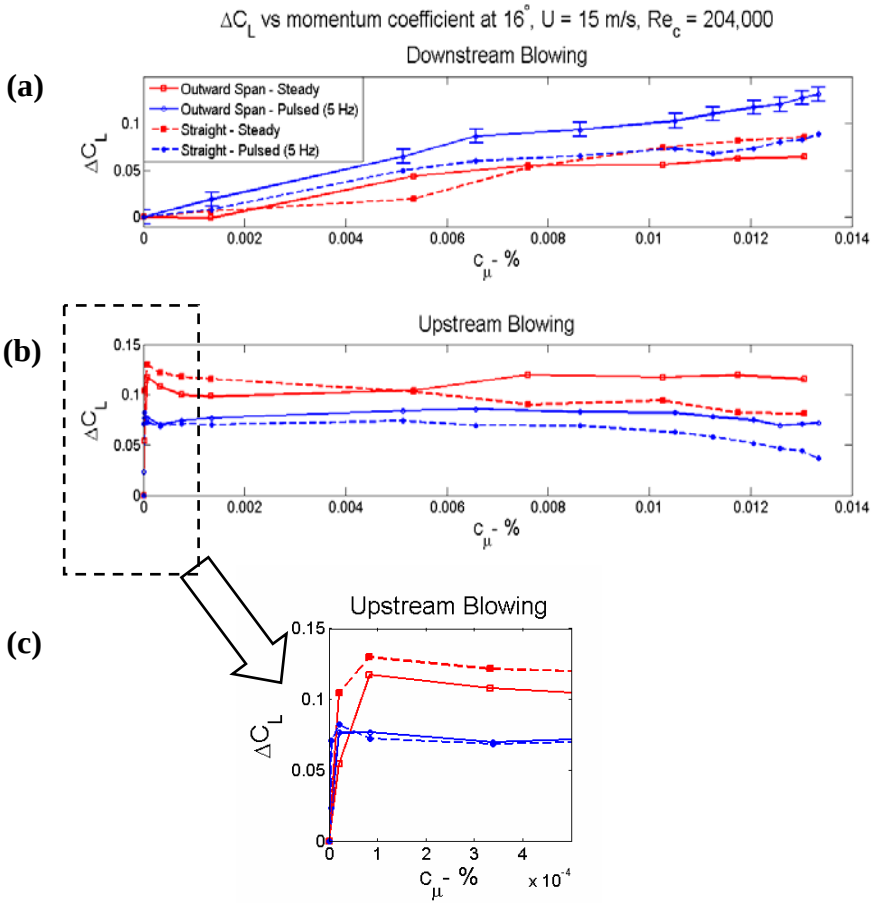

Figure 10. Effect of actuator configuration on lift increment at α = 16^{o}; (a) downstream actuation; (b) upstream actuation; (c) zoomed-in view of upstream blowing, Cμ<5x10^{-4} percent.

B. Spanwise Circulation Control

As mentioned in the Introduction, one of the main objectives of the MURI project is to gain control over the leading edge and tip vortices. Low-Reynolds number experiments suggest that this may be achieved by control of the spanwise distribution of circulation. To document the spanwise distribution of circulation we used PIV measurements at eight spanwise locations extending from the mid-span to the tip of the airfoil on both the flat-plate and NACA 0012 airfoils. Due to optical access limitations, only the flow over the top surface was recorded, so the circulation measurement was limited to the suction surface of the airfoil. Averages of the mean and r.m.s. velocity components, and Reynolds stress were computed from 100 image pairs. Since the lift at $\alpha=0^o$ is nearly zero (except for flow asymmetry caused by the airfoil support sting), the overall circulation should also be zero. However, the circulation on the upper surface will be non-zero, because of the finite thickness effect. Therefore, the circulation on the upper surface at $\alpha=0^o$ was used as a reference, and the change in circulation from the reference state associated with change in angle of attack and the effects of forcing were computed.

The change in the circulation computed from the upper surface velocity field is shown in Fig. 12 for different forcing conditions on the flat plate airfoil with upstream actuation. Both outward span and straight blowing leading edges were used. In terms of overall lift enhancement, the straight blowing actuator, operating at f=150 Hz pulsing frequency was slightly more effective than upstream steady blowing. The straight-upstream actuator configuration had the largest influence on the circulation in the mid-span region, which accounts for the largest lift enhancement. The outward-span actuation had only a minor influence on the circulation in the mid-span region of the airfoil, because the flow was directed away from the mid-span toward the tip regions. None of the actuators influenced the circulation beyond y/(b/2)=.80.

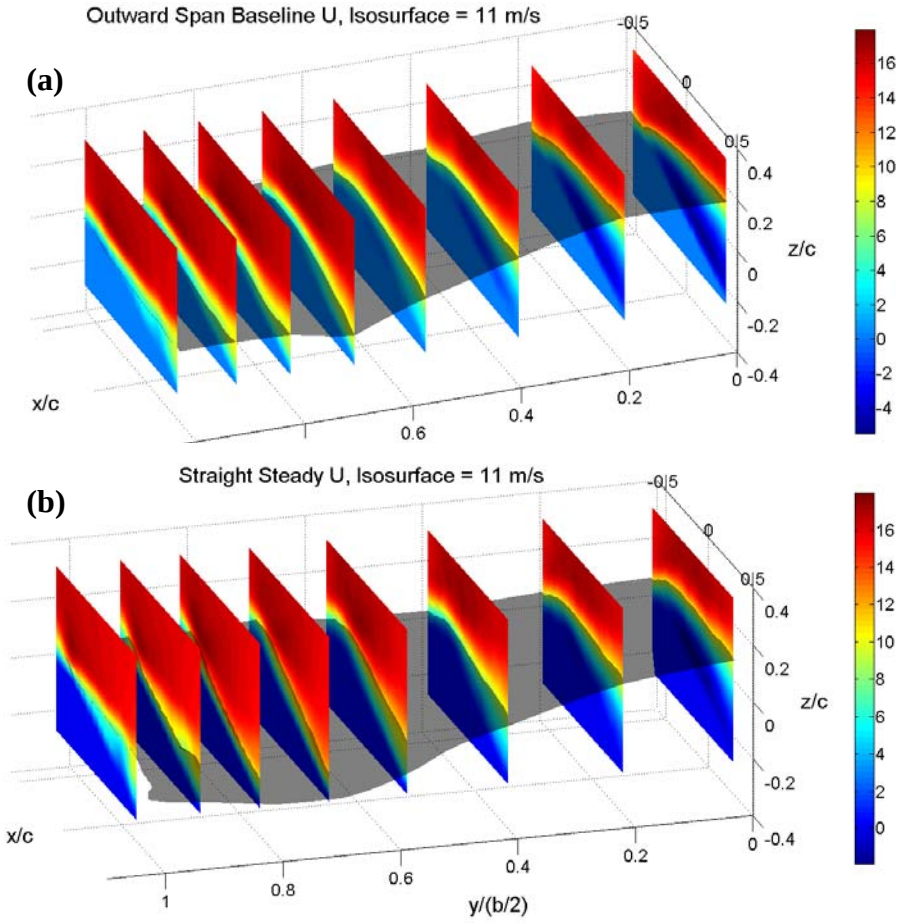

Figure 11. Iso-surface of streamwise velocity U=11m/s over flat plate airfoil, Rec =204,000. (a) baseline without actuation; (b) upstream actuation at C_μ = 8.3 x 10^{-5} percent.

Similar open-loop control experiments were conducted on an NACA 0012 airfoil at a lower Reynolds number, Re_c = 68,000. Actuators were distributed along the leading edge and tip regions in an effort to modify both the leading edge and tip vortices. In contrast to the flat plate airfoil, these actuator jets were directed downward through slots along the leading edge, in an effort to use the Coanda effect to modify the flow. PIV measurements of the velocity magnitude are shown in Figs. 13a and b. The effectiveness of a single actuator located at the mid-span of the airfoil is shown in Fig. 13b. Comparing Figs 13a with 13b, it is clear that the size of the separated flow region has been reduced with pulsed-blowing actuation at C_μ = .125 percent, and F^+=2.

The spanwise distribution of circulation measured over the NACA0012 airfoil is shown in Fig. 14. Each curve corresponds to a different actuator being activated. Actuators 1 – 4 were located along the leading edge, while actuators 4 – 6 were placed along the tip. Irrespective of which actuator was used, the circulation was primarily increased in the central span region of the airfoil, y/(b/2) < 0.5. Actuator #1 located in the mid-span region had the largest effect, but even actuator #4 located at the tip would influence the mid-span circulation.

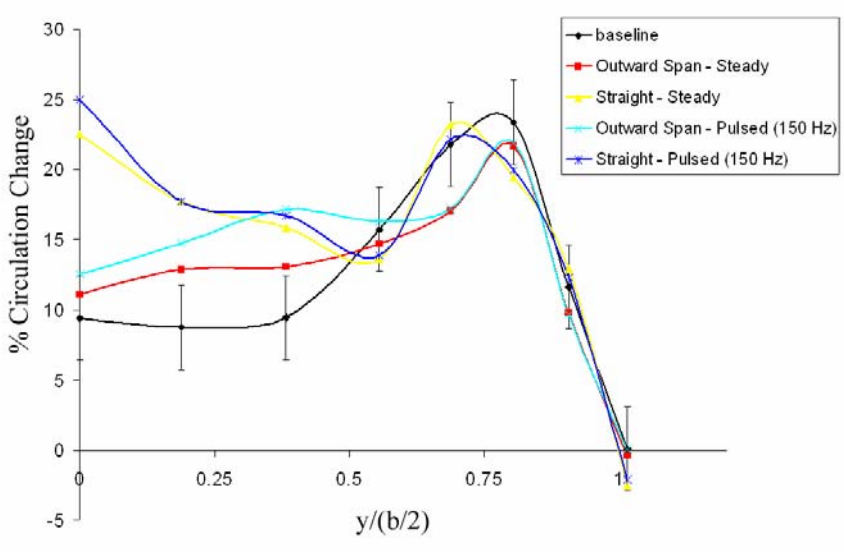

Figure 12. Percentage change in circulation change on the top surface of the flat wing. U_∞ = 15 m/s, Re_c = 204K, $\alpha = 16^o$, $C_\mu = 8.3 \times 10^{-5}$ percent.

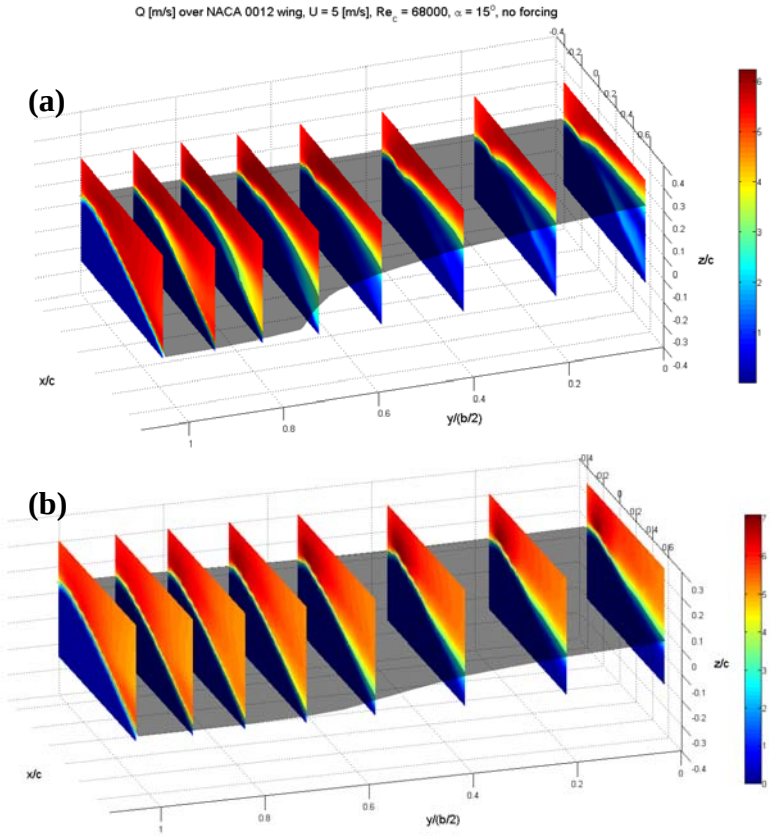

Figure 13. Contours of velocity magnitude, Q, on an NACA 0012 wing at α=15°. The Isosurface of Q = 3 m/s highlights the separated flow region. (a) baseline without forcing; (b) forced case from actuator #1 located at the mid-span, Cμ = .125 percent

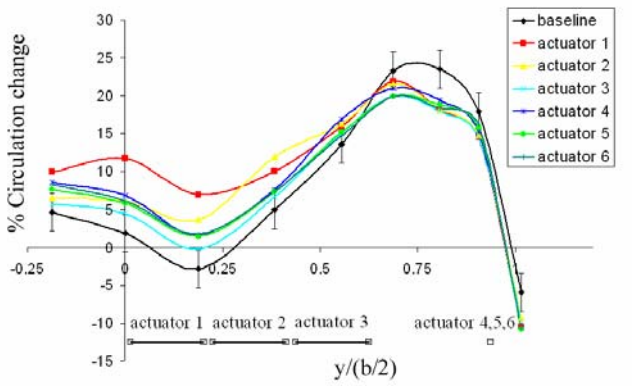

Figure 14. Percentage change in circulation on the top surface of an NACA 0012 wing referenced to the circulation at α=0°. Re_c = 68,000, α = 15°, C_μ = 0.125 percent, F^+ = 2.0.

V. Summary

The results from experiments aimed at enhancing wing performance on two finite span airfoils, a flat plate airfoil and an NACA 0012, were reported. Different approaches to actuation with steady and pulsed-blowing jet actuators were examined, as a means to gain control over the spanwise distribution of circulation. Actuation directed in the downstream direction gradually reduced the size of the separated flow region in the mid-span region of the airfoil. With upstream directed forcing, the actuation effect saturates at very low forcing levels, but does not completely eliminate the separated flow region on the airfoil. The differences in the response of the separated region to upstream and downstream forcing amplitudes are dramatic, suggesting that the physics associated with the reduction in the flow separation region are different.

Measurements of the Reynolds stress show that the maximum negative values occur along the dividing streamline over the separated flow region. When active flow control is used, a region of strong positive Reynolds stress is formed at the tip of the airfoil. The size of the recirculation region is reduced and the negative Reynolds stress region moves closer to the leading edge of the airfoil.

Changes in the spanwise distribution of circulation were achieved in the mid-span region, and these changes coincide with the reduction in the size of the separated flow. However, little change was observed in the circulation near the tip at $y/(b/2) > 0.8$.

VI. Acknowledgements

The support for this work by the U.S. Air Force Office of Scientific Research MURI (FA9550-05-1-0369) with program manager Dr. Fariba Fahroo is gratefully acknowledged. We are also appreciative of the assistance of Crystal Lybolt with support from the Illinois NASA Space Grant Consortium.

VII. References

1. Birch, J.M., Dickson, W.B., Dickinson, M.H., "Force production and flow structure of the leading edge vortex on flapping wings at high and low Reynolds numbers," *J. of Experimental Biology*, vol. 207, pp. 1063-1072.
2. Colonius, T., Rowley, C.W., Tadmor, G., Williams, D.R., Taira, K., "Closed-loop Control of leading-edge and tip vortices for small UAV," 1st Conference on Active Flow Control, Berlin Germany, Sept. 27-29, 2006.
3. Dixon, C.J., "Lift Augmentation by Lateral Blowing Over a Lifting Surface," AIAA Paper 69-193, AIAA/AHS VTOL Research, Design and Operations Meeting, Atlanta, GA, Feb. 1969.
4. Torres, G.D. and Mueller, T.J., "Low-Aspect-Ratio Wing Aerodynamics at Low Reynolds Numbers," *AIAA J.*, Vol. 42, No. 5, 2004, pp. 865-873.